

BaTiO₃-Filled Epoxy Resin Composites: Numerical Modelling of Dielectric Constants

L. RAMAJO,¹ D. RAMAJO,^{2,**} D. SANTIAGO,²
M. REBOREDO,² AND M. CASTRO^{2,*}

¹Institute of Research in Material Science and Technology (INTEMA)
(CONICET – University of Mar del Plata), Juan B Justo 4302 (B7608FDQ),
Mar del Plata, Argentina

²International Center for Computer Methods in Engineering (CIMEC, INTEC)
Güemes 3450 (S3000GLN), Santa Fe, Argentina

The influence of BaTiO₃ content on the composite dielectric properties was investigated by finite element method (FEM). This method is attractive because of its technological applications such as those in electromagnetic shields, since it allows to determine the dielectric constant of heterogeneous mediums and show or display the electric field into the material in order to understand the interfacial behaviours. The dielectric response of an anisotropic and periodic heterostructure, was evaluated and quantified by means of a quasistatic approximation using Laplace's equation which was solved by 3D FEM. The numerical calculations were confronted with experimental data. Measurements of the effective permittivity were carried out in samples prepared by dipping technique.

Keywords BaTiO₃-epoxy composite, dielectric properties, finite element method

Introduction

Polymeric composite materials, made of epoxy resin and dielectric ceramic particles, have been reported to possess interesting properties for a variety of electronic applications, such as passive electronic devices. Polymer-ceramic materials have aroused a lot of attention specially for uses in microelectronic packaging, because they can have high performances with lower costs, sizes and weights [1].

A dielectric composite is a heterogeneous mixture of at least two materials (host material or matrix, and inclusions) that have different properties, such as their permittivity and conductivity. The main advantage provided by composites is that they have unique dielectric characteristics which are different from their basic constituents. Nevertheless, due to its complexity and multi-parametric nature, the problem of predicting those characteristics has not been completely solved yet.

The most important aspect of the general problem is to relate both the microscopic characteristics of a phase (shape and size) and its macroscopic properties (permittivity and

Paper originally presented at IMF-11, Iguassu Falls, Brazil, September 5–9, 2005; received for publication January 26, 2006.

*Corresponding author. E-mail: mcastro@fi.mdp.edu.ar

**dramajo@ceride.gov.ar

conductivity) with the final properties of the material. All these properties can vary to different scales depending on constituents and manufacturing processes. The design of efficient materials with desired properties and accurate behaviours would be very important because of their potential applications in a great number of fields. Examples include electrical wires, sheathing electric paints for electromagnetic shielding, static electricity dissipation devices, current limiting thermistors, sensors, and integral capacitor devices. Except for some experimental investigations, few works [2–3] have been developed in order to model completely the dielectric behaviour of polymer-ceramic composites.

At the moment, theoretical and empirical models are being developed in order to understand and describe these composites but they often deal with specific cases. Numerical methods, such as the finite element method (FEM), seem to be a very suitable approach to describe the behaviour of these materials, because FEM does not impose restrictions to the geometry, to non-linear properties of components or to the number of phases of the composite material.

Predicting the electric field distribution in a material is the key object of all numerical models and a variety of numerical methods has been employed to solve the field problem in 2D and 3D structures. Examples are: the boundary integral method [4], the finite element method (FEM) [5], and the finite-difference time-domain method [6]. An advantage of FEM is its potential to handle the complex geometries and the non-linear properties of the components, due to the possibility of using unstructured meshes.

In this paper, a 3D FEM computer model is applied to calculate the dielectric properties of a BaTiO₃-filled epoxy resin composite. The results are reported for 20°C and 2500 Hz and they are confronted with experimental data obtained from samples prepared by a dipping technique.

Numerical Modelling

The finite element method is a numerical analysis technique in which the solution domain is discretised into smaller regions called elements, and the solution is determined in terms of discrete values of some primary field variables u (e.g. displacements in x , y z directions) at the nodes. The number of unknown primary field variables at a node is the degree of freedom at that node.

Mathematical Details

A brief description of the mathematical problem and the approach used to solve it, is described following.

The first principle of electrostatics (Laplace's equation) can be employed to compute the permittivity inside a differential domain $d\Omega$.

$$\begin{aligned} \frac{\partial u}{\partial x_i} \left(\lambda \frac{\partial u}{\partial x_i} \right) + Q &= 0 \quad \text{in } d\Omega \\ u - \bar{u} &= 0 \quad \text{on } \Gamma u \\ \lambda \frac{\partial u}{\partial n} - \bar{q} &= 0 \quad \text{on } \Gamma q \end{aligned} \quad (1)$$

where x_i are the spatial coordinates ($i = 1, 2, 3$), u is the potential distribution inside the 3-D spatial domain $d\Omega$ with a null charge density at all points, Q is a volumetric

electric-field source, λ is the electric conductivity and \bar{u} and \bar{q} are the prescribed values of potential (“essential boundary conditions”) and electric field flow (“natural boundary conditions”) on the boundaries Γ_u and Γ_q , respectively.

Variational Approaches

Each one of the three expressions in equation 1 is zero, therefore their sum also has to be zero. And so the integral form of equation 1 can be written:

$$\int_{\Omega} \left[\frac{\partial u}{\partial x_i} \left(\lambda \frac{\partial u}{\partial x_i} \right) + Q \right] dx + \int_{\Gamma_u} [u - \bar{u}] d\Gamma_u + \int_{\Gamma_q} \left[\lambda \frac{\partial u}{\partial n} - \bar{q} \right] d\Gamma_q = 0 \quad (2)$$

where dx is the differential volume and $d\Gamma$ is the differential boundary surface. Assuming that one of the boundary conditions ($u - \bar{u} = 0$ on Γ_u) is automatically satisfied by the choice of appropriated functions u on Γ_u , the second integral in eq. 2 can be removed. The variational approach starting from multiplying the equation 1 by an arbitrary residual function w ,

$$\int_{\Omega} w \left[\frac{\partial u}{\partial x_i} \left(\lambda \frac{\partial u}{\partial x_i} \right) + Q \right] dx + \int_{\Gamma_q} \bar{w} \left[\lambda \frac{\partial u}{\partial n} - \bar{q} \right] d\Gamma_q = 0 \quad (3)$$

Later, integrating eq. 3 by parts over the domain Ω , a weak form of eq. 1 can be obtained. The Green’s Formulae, a general one for such integration, is used:

$$\int_{\Omega} w \left[\frac{\partial u}{\partial x_i} \left(\lambda \frac{\partial u}{\partial x_i} \right) \right] dx \equiv - \int_{\Omega} \frac{\partial w}{\partial x_i} \left(\lambda \frac{\partial u}{\partial x_i} \right) dx + \int_{\Gamma} w \left(\lambda \frac{\partial u}{\partial n_i} \right) d\Gamma \quad (4)$$

Now it is possible to write the equation 3 as [7]:

$$- \int_{\Omega} \left[\frac{\partial w}{\partial x_i} \left(\lambda \frac{\partial u}{\partial x_i} \right) - w Q \right] dx + \int_{\Gamma} w \lambda \left[\frac{\partial u}{\partial n_i} \right] d\Gamma + \int_{\Gamma_q} \bar{w} \left[\lambda \frac{\partial u}{\partial n} + \bar{q} \right] d\Gamma_q = 0 \quad (5)$$

The second integral in eq. 5 can be rewritten using the fact that $\Gamma = \Gamma_u + \Gamma_q$, and the third integral can be separated to give:

$$\begin{aligned} - \int_{\Omega} \left[\frac{\partial w}{\partial x_i} \left(\lambda \frac{\partial u}{\partial x_i} \right) - w Q \right] dx + \int_{\Gamma_u} w \lambda \frac{\partial u}{\partial n_i} d\Gamma_u + \int_{\Gamma_q} w \lambda \frac{\partial u}{\partial n_i} d\Gamma_q + \int_{\Gamma_q} \bar{w} \lambda \frac{\partial u}{\partial n} d\Gamma_q \\ + \int_{\Gamma_q} \bar{w} \bar{q} d\Gamma_q = 0 \end{aligned} \quad (6)$$

and further, making $\bar{w} = -w$ on Γ , eq. 7 is obtained:

$$\int_{\Omega} \frac{\partial w}{\partial x_i} \left(\lambda \frac{\partial u}{\partial x_i} \right) dx - \int_{\Omega} w Q dx - \int_{\Gamma_u} w \lambda \frac{\partial u}{\partial n_i} d\Gamma_u - \int_{\Gamma_q} w \bar{q} d\Gamma_q = 0 \quad (7)$$

If the choice of u is restricted to satisfy the essential boundary conditions on Γ_u ($u - \bar{u} = 0$) the third term in equation 7 can be omitted by restricting the choice of w to functions which give $w = 0$ on Γ_u .

Approximation to Weak Formulation. The Finite Element Method FEM

Equation 7 has validity in the complete domain Ω . But Ω is a generic volume so it can be as small as one wants. It means that equation 7 is applicable both in all Ω and in finite volume fractions $\Delta\Omega$ inside of Ω .

The domain Ω shall be divided in N finite elements (finite volume $\Delta\Omega$). Then, the unknown functions u and w are approximated by the following expansions inside of each element:

$$u \approx \hat{u} = \sum_{j=1}^n N_j u_j, \quad w = \sum_{j=1}^n v_j \delta u_j \quad \text{and} \quad \bar{w} = \sum_{j=1}^n \bar{v}_j \delta u_j \quad (8)$$

where N are a set of n interpolation functions, v are a set of weighted functions and u_j are solutions of u in specified locations inside and on the boundary of the element. Different methods have been developed in order to define the weighted functions v_j . Here, the Galerkin's method, the most accepted of them, has been adopted. It considers $v_j = N_j$, that means the original shape functions N are used as weighting. Finally, equation 7 is written as:

$$\int_{\Delta\Omega} \frac{\partial N_j}{\partial x_i} \left(\lambda \frac{\partial N_k}{\partial x_i} u_k \right) dx - \int_{\Delta\Omega} N_j Q dx - \int_{\Delta\Gamma_q} N_j \bar{q} d\Gamma_q = 0 \quad (9)$$

where sub index j and k are 1, 2, . . . n.

It is possible to obtain a complete description of u from u_j and the interpolation functions N. For this purpose, the implementation of the finite element method consists in selecting an appropriate polynomial interpolation function set, N, dividing the spatial domain Ω in finite elements and applying the equation 9 in each element in order to calculate the nodal values u_j of the field u. These values must match the imposed boundary conditions in the element frontier. Then, the solution of u inside of the element can be obtained by using equation 8. Following this way, the integral equation 9 must be transformed in a matrix equation for every finite element in the unit cell (Fig. 1). After that, all matrixes are connected by means of their common nodes, and a non-linear equation system is obtained. It is numerically solved, and the solution of u in nodes of the unit cell is known.

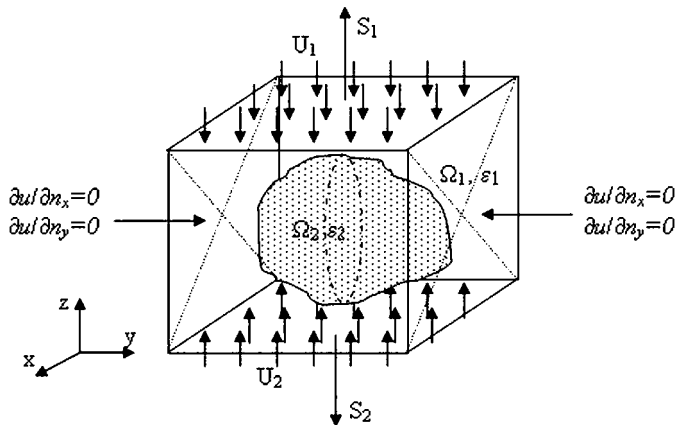


Figure 1. Scheme of the unit cell of a two-component periodic composite material and the assumed boundary conditions.

The effective permittivity ε , in the direction corresponding to the applied field, can be calculated by applying an energy balance between the surfaces S_1 and S_2 , using the following relation:

$$\int_S \varepsilon_i \left(\frac{\partial u}{\partial n} \right)_i ds = \varepsilon \frac{U_2 - U_1}{e} (S_1 + S_2) \quad (10)$$

where $U_2 - U_1$ denotes the potential difference imposed in the z-direction, e is the composite thickness in the same direction, ε_i is the permittivity of the surface region and S is the area of surface where the field is applied.

Computational Procedure

The unit cell was composed by a matrix which had n spherical particles of BaTiO₃ inside it. Particles were placed in an equidistant way, filling all the matrix. Boundary conditions were an electrical potential difference of 1V in the z-direction and potential gradients equal to zero in the x and y directions ($\partial u / \partial n_x = 0$ and $\partial u / \partial n_y = 0$). The particle size (radius) was changed to study the influence of BaTiO₃ particles volume fraction in the composite.

A symmetric array of 9 spheres in a face centred cubic node configuration (FCC) was selected to perform the analysis. Table 1 shows the dielectric properties of the two constituents at 25°C and 2500 Hz.

In order to generate the data files for geometry, boundary conditions and material properties, a program was developed. Also, previously developed general purpose finite-element software was used to assemble and solve the non-linear system. This program gives the possibility of choosing between a great numbers of boundary conditions as well. Both software allow the calculus of the effective permittivity and the potential distribution.

Experimental Procedure

Epoxy DER 325 (Dow Chemical) was chosen because of its good dielectric properties (Table 1). DEH 324 (Dow Chemical) was used as the curing agent (12.5 phr) and commercial BaTiO₃ (TAM Ceramics Inc.) was used as the filler.

The mixed solution was placed in a glass substrate with gold electrodes deposited by dc-sputtering, using a dipping technique (at a rate of 3 cm/min) and cured at 100°C for 2 hours. A THF concentration of 60 wt% was introduced to reduce the viscosity of the mixture. Filler fractions were around 20 to 50 vol%. Dielectric measurements were performed using a Hewlett Packard 4284A Impedance Analyser in the frequency range 20 Hz to 1 MHz.

Table 1
Values for real permittivity and loss tangent at
25°C and 2500 Hz

Constituent	ε'	$\tan \delta$
BaTiO ₃	2400	0.0505
Epoxy	4.15	0.0082

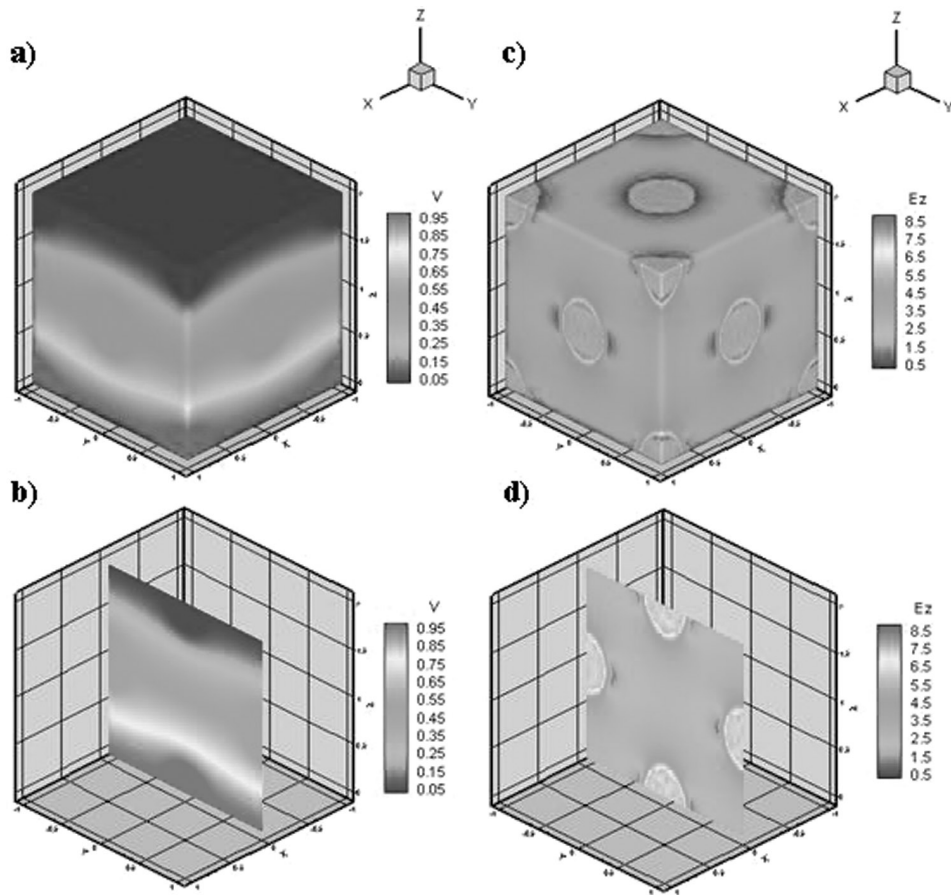


Figure 2. Potential and electric field distributions around (a, c) and into (b, d) the lattice with a volume fraction of 5% of particles. (See Color Plate XV)

Results and Discussion

Figure 2 shows the potential and electric field distributions across a hypothetical composite with 5 vol% of filler. Pictures (a) and (b) show the potential distribution around, and into the lattice, while pictures (c) and (d) represent the electric field distribution. A clear distortion around the inclusions is observed, together with a slight potential reduction inside them. This behaviour agrees with the expected effects generated by the electric field in dielectric materials [8]. On the other hand, it can be seen that the electrical field shows smaller particle-particle interaction in a model with low filler amount. In addition, its intensity has a local growth inside the ceramic material. This result agrees with the increase of permittivity experimentally found for high filler composites.

The FEM solution for a composite with 70 vol% of filler is shown in Fig. 3. Pictures (a) and (b) show the potential profiles around and inside the lattice, while pictures (c) and (d) represent the electric field distribution. A higher electric field inside the particles and a stronger particle-particle interaction are also observed in this case. High filler composites generate a great distortion over the potential and the electric field, principally where the particles are closer.

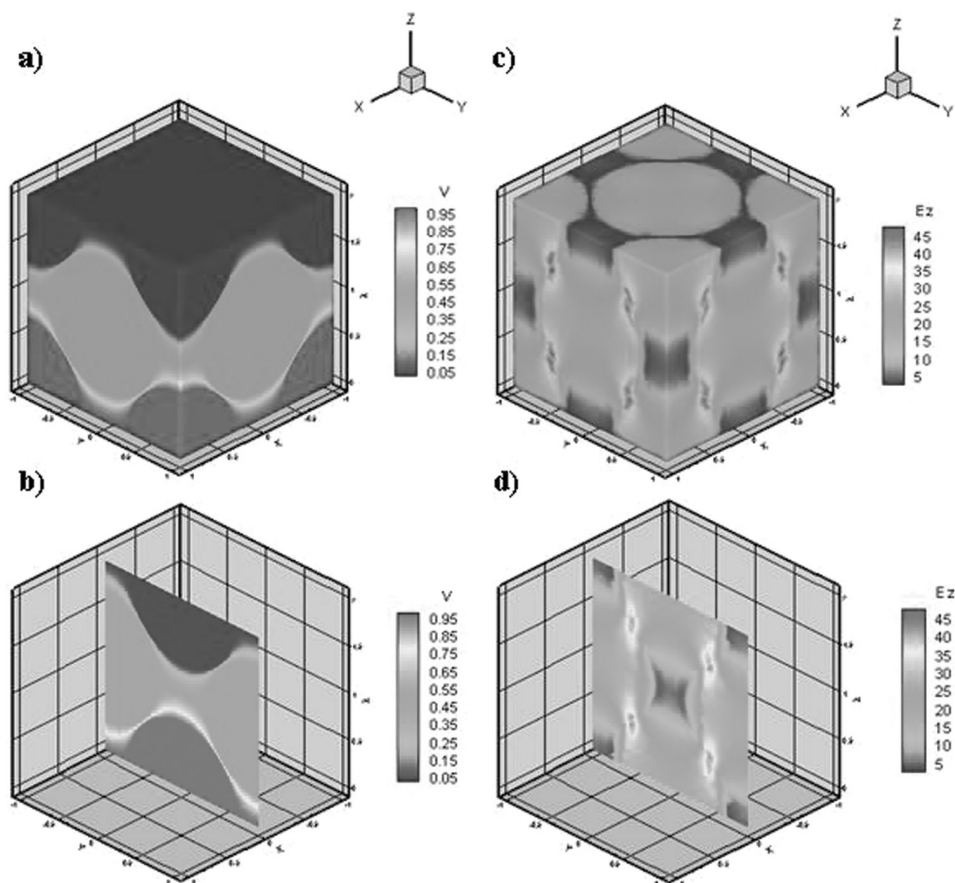


Figure 3. Potential and electric field distribution around (a, c) and into (b, d) the FCC lattice. Simulation made with 70% of particles volume fraction. (See Color Plate XVI)

The results show that when the distance between particles decreases, a particle experiences the effect of local fields induced by its closer neighbor particles. For volume fractions around 72% (corresponding to the limit of touching spheres), the highest interaction effects and the highest dielectric constant values were obtained.

In Fig. 4 the electrical field on a body face for a composite with 5 vol% of filler is represented with vectors. This case illustrates the effects of morphology over the potential gradients through the composite. As it can be seen in the figure, the electric field flow turns to the particles following the easier path provided by the inclusions. Thus, if the particle volume fraction increases, the electric field will grow and subsequently higher dielectric constants can be produced.

In Fig. 5, experimental measurements of permittivity are shown along with FEM simulation results for composites with low loading concentration. Results from two theoretical models (Maxwell's model [9] and Rayleigh's model [10]) are also included. Maxwell's model considers that the composite is made of non-interacting spherical particles in a random configuration, and that they are inserted in a homogeneous dielectric medium [9], while Rayleigh's model improves Maxwell's model by considering the interaction of the particles through a regular array [10].

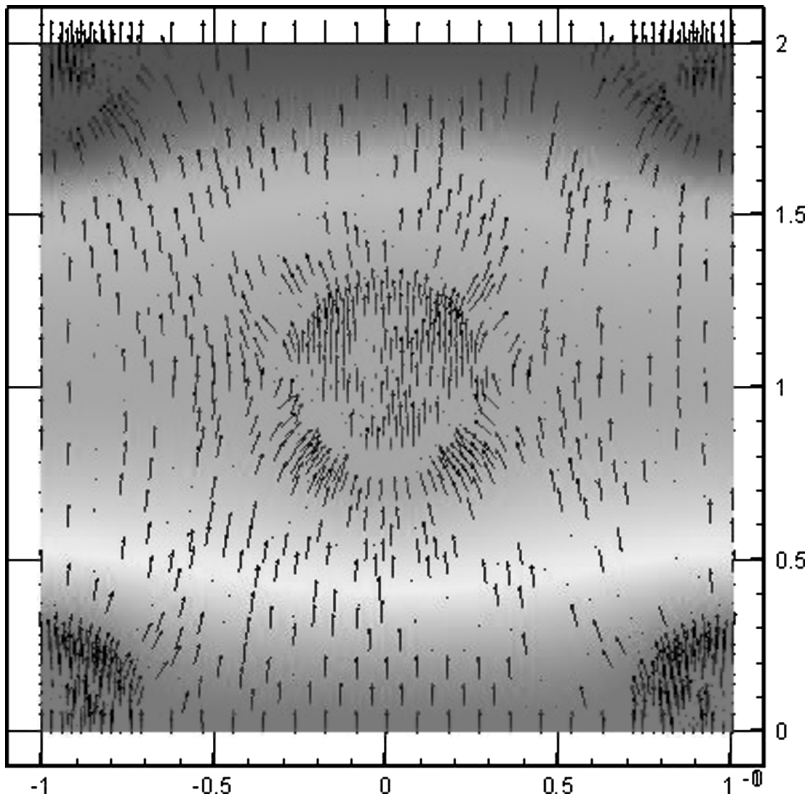


Figure 4. Map of electric fluxes in a composite with 5 vol% of filler. (See Color Plate XVII)

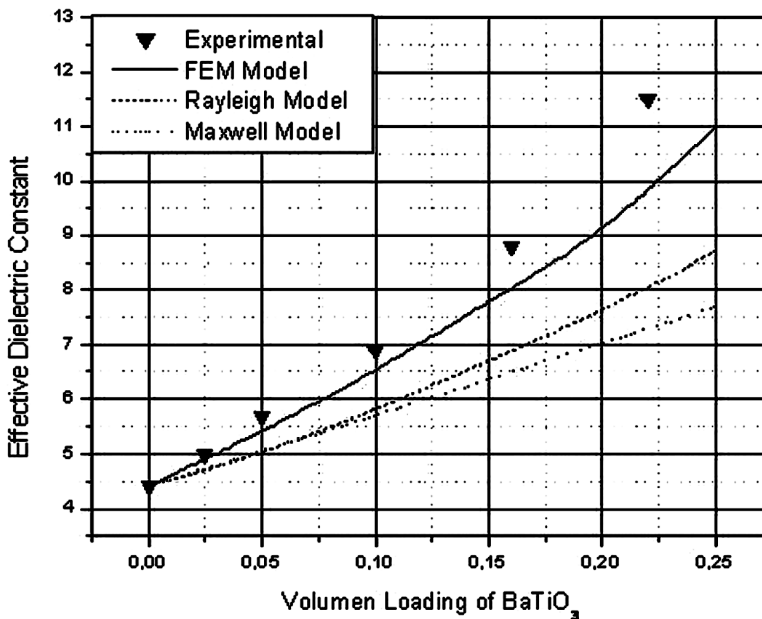


Figure 5. FEM prediction (solid curve), Rayleigh's model (dashed line), Maxwell's model (dotted curve) and experimental results (solid dots) of the dielectric constant (low volume fraction zone).

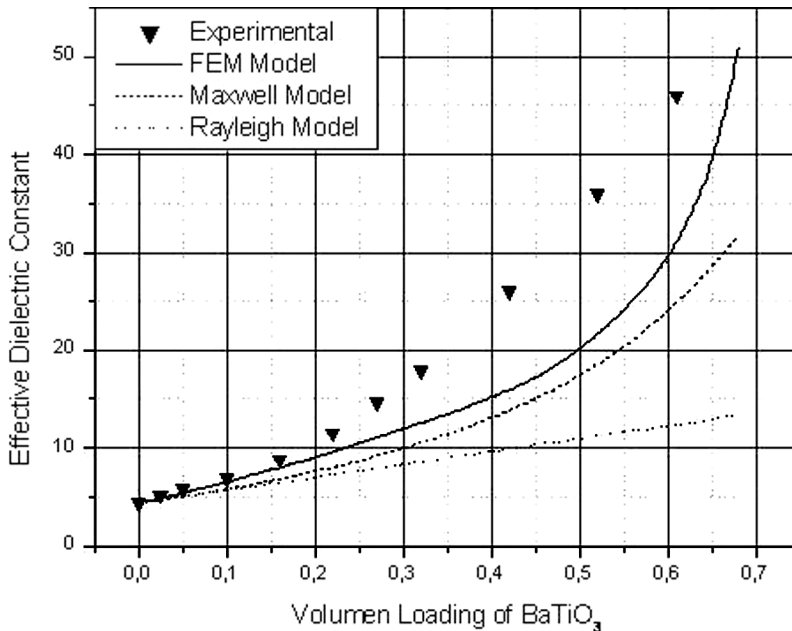


Figure 6. FEM predictions (solid curve), Rayleigh's model (dashed curve), Maxwell's model (dotted curve) and experimental results (solid dots) of the dielectric constant vs. BaTiO₃ concentration.

It can be seen that BaTiO₃ particles generate an increase in the permittivity in all the curves. However, the FEM model gives a much better prediction of permittivity than Maxwell and Rayleigh's models. The differences between experimental results and FEM predictions are less than 5% for samples with BaTiO₃ concentrations less than 10 vol%. For concentrations between 10 and 25 vol%, differences grow from 10 to 25%. Rayleigh's model performance seems to be better than the one of Maxwell's, since it considers the existence of particle interaction. Nevertheless, these theories are not helpful to approach this real system.

On the other hand, FEM model makes inaccurate predictions for high BaTiO₃ concentrations. As it can be seen from Fig. 6, the error increases with the BaTiO₃ content until 45 vol% at which a maximum difference between the model and the experimental results is reached (around 45% error). After that, the error starts to decrease as a result of a higher particle interaction while the BaTiO₃ concentration approaches to the maximum packaging threshold. The differences between FEM results and the experimental behaviour can be attributed to the particle-particle contact and to the real diameter distribution, which were not considered in the model. An improvement could be obtained by incorporating a more representative sphere-diameter distribution, introducing smaller particles inside the octahedral and tetrahedral domains, defined among the bigger particles, in the FCC structure.

Conclusion

A numerical and experimental investigation of composites of epoxy/BaTiO₃ was made. Results of numerical simulation using a FEM model were confronted with experimental results and the following conclusions were reached:

1. The implemented numerical model using the finite element method reproduces the experimental behaviour much better than Maxwell and Rayleigh approaches.
2. The results from the FEM model suggest that the electric field is strongly influenced by the particle-particle distance. In this way, the electric field distribution for volume fractions near to maximum-packaging threshold presents higher interaction and corresponds to the highest dielectric constant values.
3. In general, the potential and electric field distributions could be represented by the model. However, it can not represent very well the behaviour of high concentration composites. A model with a more complex geometry including the effect of particle-particle contact could improve the fitting of experimental data.

Acknowledgments

This work was supported the National Council of Science and Technology of Argentina (CONICET) and ANPCyT/FONCyT PICT 14738 (BID 1201/OC-AR). It was also achieved thanks to material donation from Dow Chemical Argentina due to management of Ariadna Spinelli and Alfredo Fahnle.

References

1. K. Uchino and S. Takahashi, Dielectric Ceramic Materials. *Ceramic Transactions* **100**, 455–468 (1999).
2. A. Beroual and C. Brosseau, Comparison of dielectric properties determined from a computational approach and experiment for anisotropic and periodic heterostructures. *IEEE Trans. Dielectrics EI* **8**, 921–929 (2001).
3. Y. Serdyuk, D. Podoltsev, and S. Gubanski, Numerical simulation of dielectric properties of composite material with periodic structure. *J. Electrostatics* **63**, 1073–1091 (2005).
4. A. Beroual and C. Brosseau, Computational electromagnetics and the rational design of new dielectric heterostructures. *Progress in Materials Science* **48**, 373–456 (2003).
5. R. Otín, El método de los elementos finitos aplicado a problemas electromagnéticos en el dominio de la frecuencia. Barcelona: CIMNE (2004).
6. K. K. Karkkainen, A. H. Sihvola, and K. I. Nikoskinen, Effective permittivity of mixtures: numerical validation by FDTD method. *IEEE Trans. Geosci. Remote Sensing* **38**(3), 1303–1308 (2000).
7. O. C. Ziniewicz and R. L. Taylor, The finite element method. Vol I. London: MacGraw Hill Book Company (1989).
8. J. M. Albella Martin and J. M. Martinez Duart, Física de dieléctricos. Spain: Boixareu Editores (1984).
9. D. H. Yoon, J. Zhang, and B. I. Lee, Dielectric constant and mixing model of BaTiO₃ composite thick films. *Materials Research Bulletin* **38**, 765–772 (2003).
10. N. E. Frost, P. B. McGrath, and C. W. Burns, Effect of filler on the dielectric properties of polymers. Conference Record of the 1996 IEEE International Symposium on Electrical Insulation. Montreal. Quebec. Canada. 300–303 (1996).